

IMPACT OF THE SPATIAL AND TEMPORAL VARIABILITY OF SNOWPACK CONDITION ON INTERNAL LIQUID WATER FLUXES

Eole Valence¹ and Michel Baraer¹

ABSTRACT

The seasonal snow cover plays an important hydrological role in cold regions. The terrestrial cryosphere, which is highly sensitive to climate change, raises questions about how the evolution of snowpack characteristics will affect water resources in non-mountainous environments. The present paper presents the first results from a multimethod study on the interconnections between the snowpack structure and its internal liquid water fluxes. Fieldwork for the study was conducted at the experimental watershed of Ste-Marthe QC, Canada (BVE Ste-Marthe during winter 2020–2021). We combined the application of drone-based high-frequency ground-penetrating radar (GPR), near-infrared (NIR) and red-green-blue (RGB) photogrammetry, time-domain reflectometry (TDR moisture), stable isotopes of water, and monitoring of snowpack properties throughout the winter season. We focused on weekly drone-based GPR surveys conducted over a flat and a sloped zone of the study site. Two-way travel time (TWT) transects extracted from the radargrams are superimposed to snow depth from HD digital elevation models to compute permittivity profiles. Results show differences in hydrological response to the mild episode on March 11. The use of drone-based GPR for the study of spatiotemporal snowpack properties variability appeared extremely promising (KEYWORDS: rain-on-snow, UAV photogrammetry, high-frequency GPR, drone-based GPR, effective permittivity).

INTRODUCTION

By storing and then releasing solid precipitations, the seasonal snowpack gives shape to the annual hydrograph in cold regions. In addition, because snowpack characteristics affect liquid water pathways and residence time, they have major implications on the distribution of meltwater to groundwater recharge, moisture storage, and surface runoff. During rain-on-snow (ROS) events, snowpack properties influence the speed and amount of liquid water flowing out of the snowpack to the surface drainage system, with ice jams and winter floods as potential consequences. Observations and climate models show an increase in ROS frequency in many cold regions across the Earth. This trend shall trigger increases in the frequency of winter floods and ice jams. A good understanding of the processes and parameters influencing liquid water outflow from the snowpack is required to better anticipate the hydrological consequences of the increasing frequency of ROS events.

In a more general perspective, reliable projections of climate change affecting the hydrosphere in northern regions require hydrological models that account for appropriate hydrological processes. Developing such hydrological models calls for a good understanding of snow hydrology in non-mountainous environments. However, studying snow hydrology is difficult in non-mountainous regions where the maximum seasonal cover barely reaches one meter. Moreover, in regions where snowpack structure fluctuates over the entire winter, such as those affected by frequent rain on snow events, capturing the snowpack structure/flow through interconnections requires winterlong observations through nondestructive methods. Such observations are difficult to perform, as they are conducted in harsh environments, including high amplitudes in air temperature fluctuations and mixed-precipitation events.

The main objective of the present article is to present results from a multimethod study on the interconnections between the snowpack structure and its internal liquid water fluxes. This research took place at the experimental watershed of Ste-Marthe QC, Canada during winter 2020–2021. We applied an original combination of methods to characterize snowpack structure evolution in time and space. The results presented here cover drone-based GPR surveys, drone-based photogrammetry, and field observations such as sequential sampling in snow pits.

STUDY SITE

The study site is at the main station of BVE Ste-Marthe, located around 70 km west of Montréal, Canada (45.423907N, 74.284073W, 120 m elevation). The main station is in a forest clearing of around 200 m² (Figure 1).

Paper presented Western Snow Conference 2021

¹ Eole Valence, École de Technologie Supérieure, Montréal, eole.valence.1@ens.etsmtl.ca

¹ Michel Baraer, École de Technologie Supérieure, Montréal, Michel.Baraer@etsmtl.ca

Two different transects were considered for the GPR and photogrammetric surveys: one over a flat section and the other over a sloped section. The main station hosts an automatic weather station (AWS) that measures multiple hydroclimatic variables among which we find snow depth, air temperature, ground and snowpack internal temperature, precipitation amounts, and snowpack outflow at the snow–ground interface.

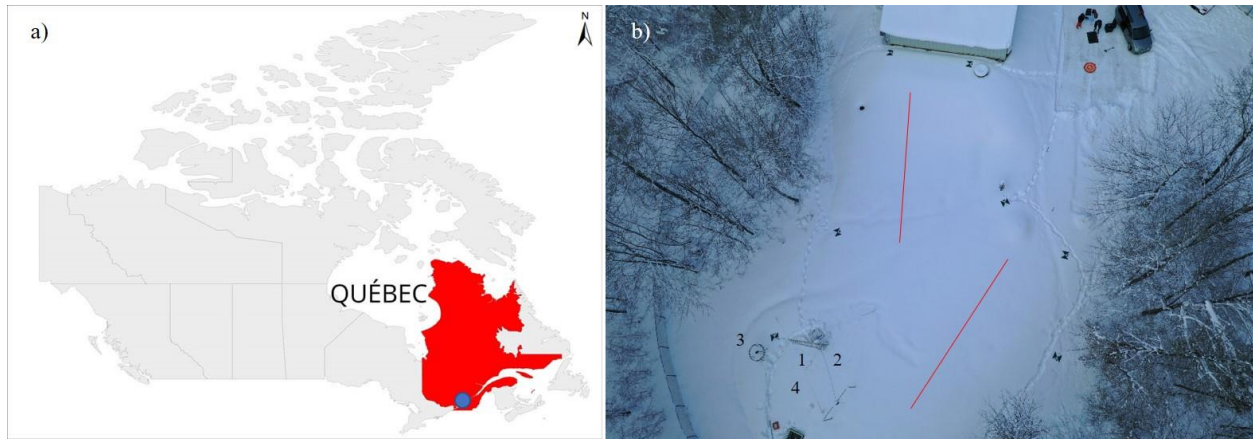


Figure 1. Study site. a) Location of the BVE Ste-Marthe in Canada. b) Overview of the main station; red lines represent the two studied transects. Numbers identify devices of interest for the present study: (1) sonic sensor, (2) ground and snow temperature sensors, (3) shielded precipitation gauge, and (4) snow lysimeter.

Winter 2020–2021 was characterized by a limited maximal snow depth (0.7 m) and only three ROS events (Figure 2). As our objective is to study the snowpack structure/flow through interconnection, we focused on the mild episode (including a minor ROS event) from March 9 to 12. Three survey dates were selected to study that episode: March 5, 12, and 19. March 5 represented the end of the accumulation period. Snow depth was less than 10% lower than the year maximum, the air temperature stands below -10 degrees, and the previous mild episode occurred more than five days before. Lysimeter outflow, temperature at the snow–ground interface, and temperature within the snowpack indicated that at least part of the snowpack is cold.

March 12 marked the last day of the mild episode. Snow depth decreased by almost 30% since the last survey, and a flow of liquid water has been detected by the lysimeter on March 11. On March 12, the air temperature gradually decreased to zero, and no precipitation was recorded. The ground, snowpack, and snow–ground interface temperatures were all at the melting point, indicating that the snowpack is probably at maturation.

Between March 12 and 19, a winterlike precipitation-free condition prevailed. This period was

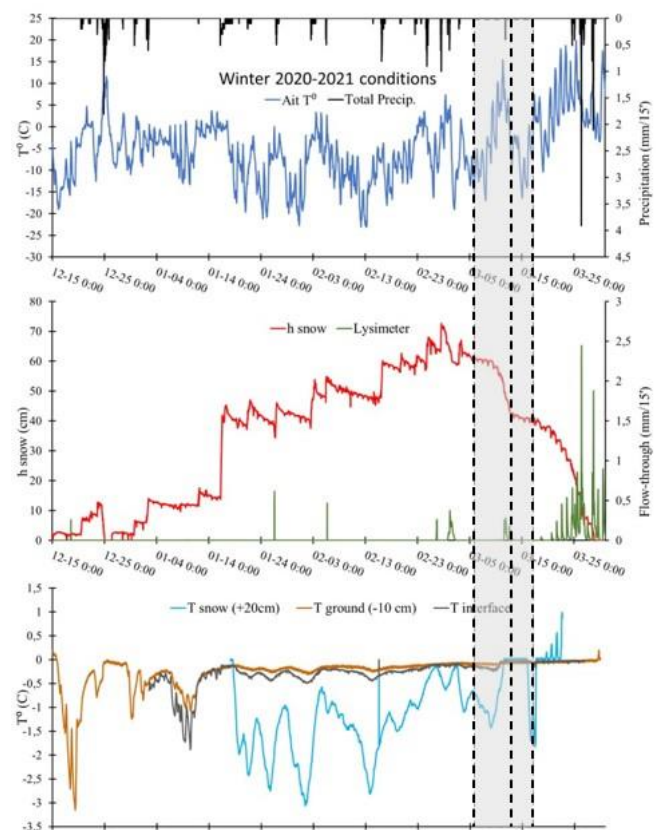


Figure 2. Winter 2020–21 conditions monitoring. Dash lines indicate GPR survey days selected for the study. The gray area represents the studied period. Time series names in the legend stand for: *Air T*: air temperature taken at 2 m height; *Total precip*: total precipitations; *h snow*: snow depth; *Lysimeter*: liquid water outflow at the snow–ground interface; *T snow (+20 cm)*: the internal snowpack temperature at 20 cm above the ground; *T ground (-10 cm)*: the ground temperature at 10 cm below the ground surface; and *T interface*: temperature at the snow–ground interface.

characterized by continuous subzero air temperatures, snow depth stability, and no outflow at the base of the snowpack. On March 19, the day the GPR survey was performed, snowpack temperature dropped at -2°C , and the snow-ground interface showed a slight tendency to fall below the freezing point.

In summary, the study period covered a transition from a cold to a wet snowpack ending with at least a partial cooling of the snow cover.

METHODS

From each survey day, the flat and sloped transects were characterized by both snow depth and effective permittivity profiles. The effective permittivity of the snowpack is liquid water content (*LWC*) and is mainly snow density dependent. In dry cold conditions, effective permittivity can be considered as a proxy for snowpack bulk density. The effective permittivity profiles for our two studied transects were created by combining outputs from two nondestructive and noninvasive methods: unmanned aerial vehicle-based (UAV) photogrammetry and UAV-based high-frequency ground-penetrating radar (GPR).

Survey Type 1

UAV-based photogrammetry was performed using a Mavic 2 Pro drone (DJI) upgraded with an improvement kit (TopoDrone) Post Processed Kinematic (PPK) corrections based on RS2 (Reach) global navigation satellite system (GNSS) base station records. The snow depth H_s of the studied transects was determined using the geographic information system software ArcGIS (ESRI) by subtracting a snow-free digital elevation model (DEM) from those produced from images collected the same day as the GPR survey (Figure 3). The snow-free DEM was created by

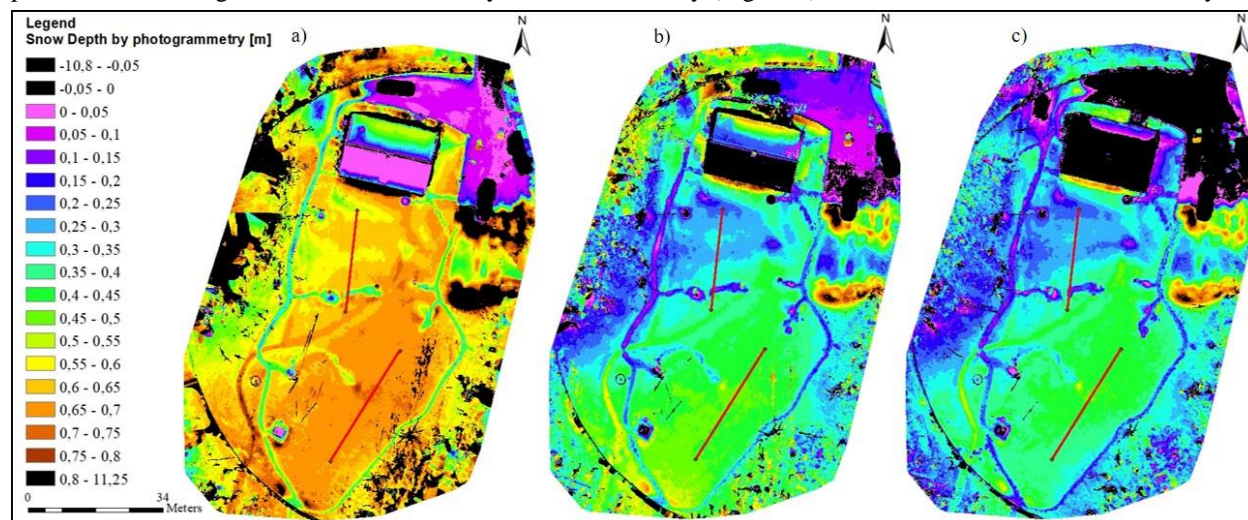


Figure 3. DEMs of snow cover by HD photogrammetry for the three field operations, red lines indicate the two studied transects. a) March 5. b) March 12. c) March 19.

flying the Mavic on April 6, just after the complete disappearance of the snow cover. Photogrammetry was performed with Pix4D software and then validated with a ground control point geolocalized using a 7700B GNSS (KlauPPK). Figure 3 shows the evolution of the snow cover over the studied period. All DEMs present a comparable repartition of the snow cover over the study site; the slope area showed shallower snow on the ground than the flat one. This confirms the evolution of the snow depth measured at the AWS and presented in Figure 2. The high level of ablation and/or settling between March 5 and 12 was ubiquitous while changes between March 12 and 19 were less pronounced.

Survey Type 2

UAV-based high-frequency GPR surveys were performed with a Zond 1.5GHz GPR (Radar System Inc.) carried by a Matrice 600 Pro drone (DJI). PPK corrections were performed by mounting the 7700B GNSS on the Matrice 600 Pro. The RS2 base station was used as a reference here as well. For each survey, radargrams were produced both for the flat and sloped areas. The radargrams were treated using Prism2 software (Radar System Inc.). The posttreatment to all radargrams consisted of a background removal filter, a time delay offset compensation, and the application of a gain function. Layer identification was performed using the observed snow pit stratigraphy as

reference. The identification was processed automatically if possible and manually if the layer boundaries were not clear enough for the algorithm (see example in Figure 4).

Data from both surveys were combined to calculate the velocity of the electronic wave (v) within the snowpack by using the following equation:

$$v = \frac{Hs}{(TWT/2)} \quad (1)$$

with TWT being the two-way travel time of the wave within the snow.

The velocity was then used to determine the effective permittivity of the snow cover ϵ_{eff} :

$$\epsilon_{eff} = (v/c)^2 \quad (2)$$

with c representing the speed of light in a vacuum (0.3 m/ns).

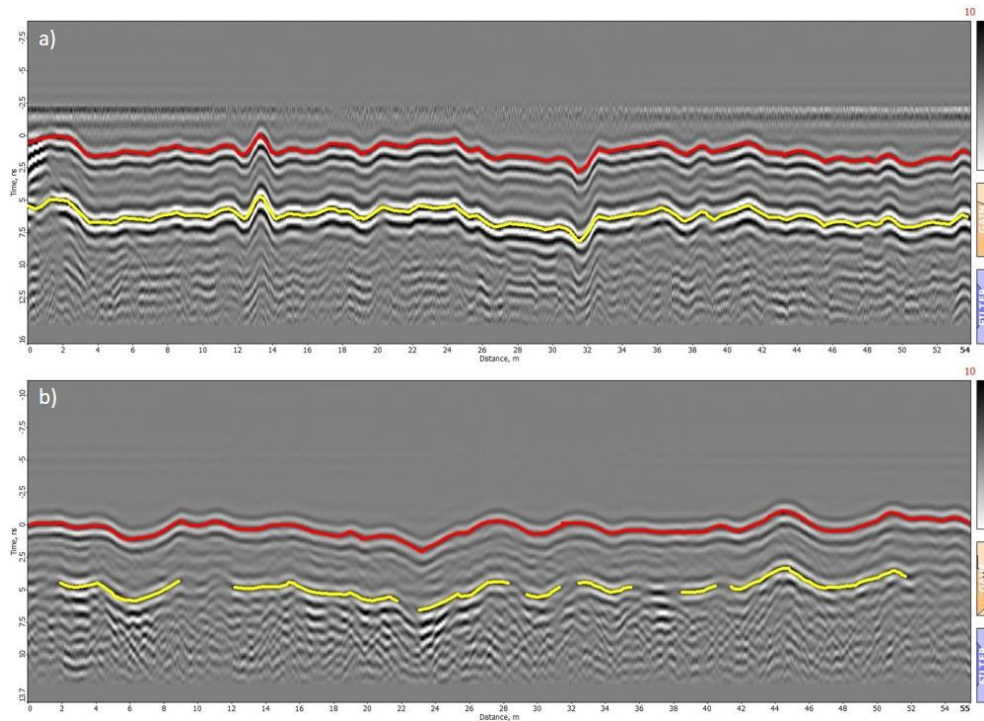


Figure 4. Example of 1.5 GHz GPR radargrams. a) Survey realized over the flat area, March 5 (dry conditions). b) Same transect as a) but surveyed on March 12 (wet conditions).

RESULTS AND DISCUSSION

Snow depth and effective permittivity profiles are shown in Figure 5. On March 5, both the flat and sloped areas show comparable levels of effective permittivity. Both profiles are stable in space, the effective permittivity showing uninterrupted, almost variation-free values. The minor difference in snow depth of those dry snowpacks indicates a slightly lower snow water equivalent (SWE) in the slope compared to that of the flat area.

In the measurements for March 12, we observed the flat and sloped transects reacted differently to the mild/wet episode of the previous days. Both areas exhibited a rise in effective permittivity and a decline in snow depth. Both areas showed gaps in effective permittivity profiles too. Those can be explained by the presence of liquid water in the snowpack. The 1.5 GHz GPR, which has a low penetration capacity, is affected by layers of high effective

permittivity, making the reflection from the ground surface undetectable. Dissimilarities between areas were observed in both effective permittivity and snow depth profiles. The flat-area effective permittivity remains stable with distance while the sloped one showed more variations. The general increase in effective permittivity was higher in the sloped than in the flat transect. As the sloped transect exhibited a more pronounced decrease in snow depth than the flat area,

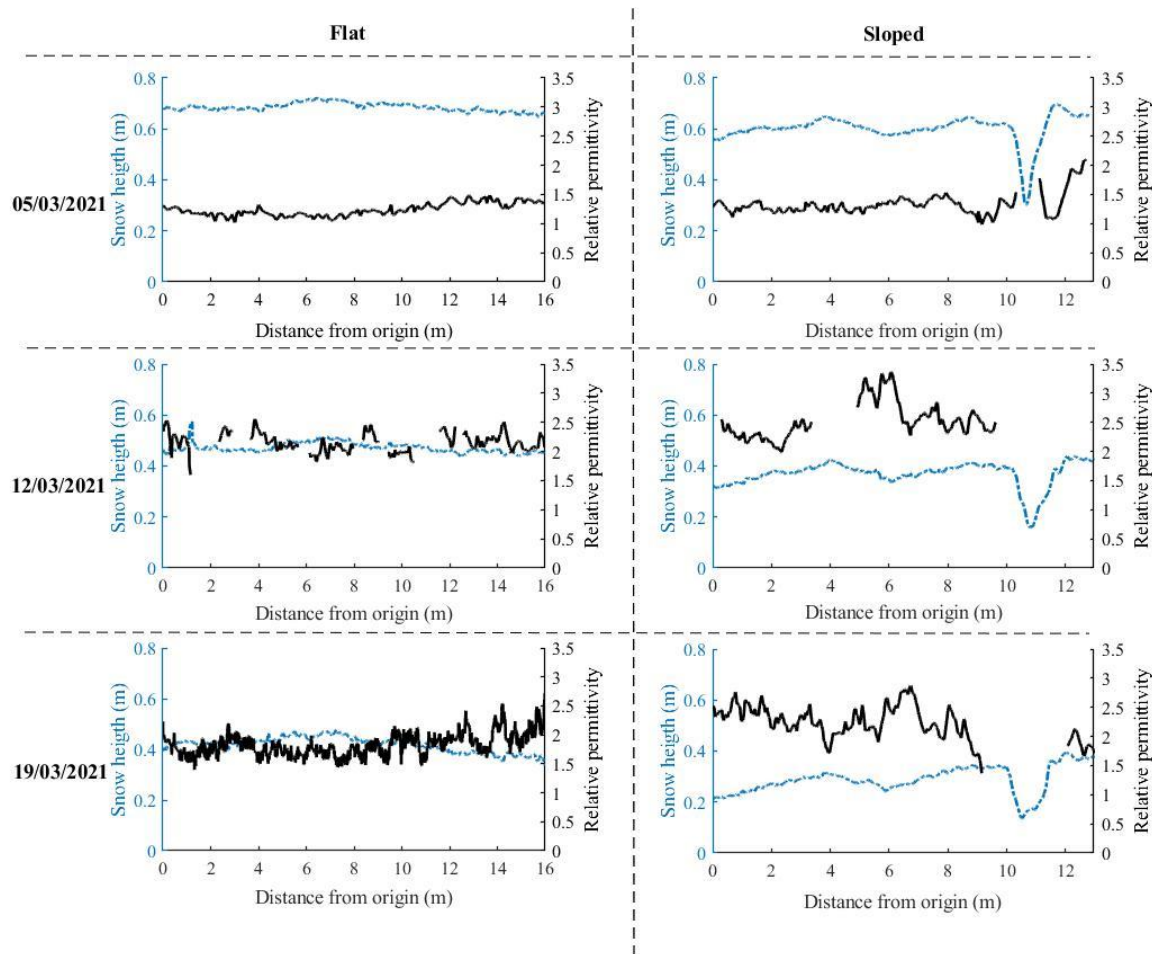


Figure 5. Effective permittivity and snow depth calculated for the flat and the sloped transects on March 5, March 12 and March 19.

it is unfortunately not possible at that stage to conclude whether liquid water content differed between those two areas. On March 19, the snow depth in the flat transects remained almost unchanged compared with the one collected on March 12, while the effective permeability, still relatively stable with distance, decreased to a level between those of March 5 and 12. The sloped area exhibited a decrease in effective permittivity, the magnitude of which is comparable with that of the flat area. The variability with distance remained higher in the sloped section. The main difference between the two March 19 profiles is in snow depth. The sloped transect showed a more pronounced decrease in slope than in the flat area. As no fresh precipitations were recorded between March 12 and 19, the decrease in permittivity in both transects can be interpreted as a decrease in LWC, which could have occurred together with snow densification in the sloped area (snow depth decrease).

CONCLUSIONS

Results showed that:

- During winter 2020–2021, the snowpack on the flat and slope surface exhibited comparable behaviors over the accumulation period as seen on the March 5 profiles but reacted differently over the studied ablation episode.

- Drone-based 1.5 GHz GPR coupled with HD photogrammetry is a well-adapted method to winterlong repetitive measurements of snowpack conditions (structure/density and moisture content). In the present study, they allowed the evolution of effective permittivity in space and time, providing valuable information on snowpack density and/or LWC evolution.

In the coming months, this analysis will be extended to the entire dataset and compared with other sources of information such as TDR measurements to extract additional insights into the snowpack structure/flow through interconnectivity during winter 2020–2021 winter at the main station of BVE Ste-Marthe, QC.

REFERENCES

Bühler Y., Adams M., Bösch R., Stoffel A. 2016. Mapping snow depth in alpine terrain with unmanned aerial systems (UASs): Potential and limitations. *The Cryosphere*, 10:1075-1088.

Fierz C., Armstrong R. L., Durand Y., Etchevers P., Greene E., McClung D. M., Nishimura K., Satyawali P. K., Sokratov S. A. 2009. The International Classification for Seasonal Snow on the Ground. *IHP-VII Technical Documents in Hydrology* N°83, IACS Contribution N°1, UNESCO-IHP, Paris.

Lundberg A., Gustafsson D., Stumpp C., Klöve B., Feiccabrino J. 2016. Spatiotemporal Variations in Snow and Soil Frost—A Review of Measurement Techniques. *Hydrology*. 3:28.

Mas A., Baraer M., Arsenault R., Poulin A., Préfontaine J. 2018. Targeting high robustness in snowpack modeling for Nordic hydrological applications in limited data conditions. *Journal of Hydrology*, 564:1008–1021.

Paquette A. 2020. Hydrological behavior of an ice layered snowpack in a non-mountainous environment. Master thesis, École de technologie supérieure, QC, Canada.

Webb R. W., Wigmore O., Jennings K., Fend M., Molotch N. P. 2020. Hydrologic connectivity at the hillslope scale through intra-snowpack flow paths during snowmelt. *Hydrological Processes*, 34:1616–1629.